

Characteristics of thunderstorms relevant to the wind loading of structures

Giovanni Solari^{*}, Massimiliano Burlando^a, Patrizia De Gaetano^b
and Maria Pia Repetto^c

*Department of Civil, Chemical and Environmental Engineering (DICCA),
University of Genoa, Via Montallegro, 1, 16145 Genoa, Italy*

(Received January 2, 2015, Revised April 15, 2015, Accepted April 21, 2015)

Abstract. “Wind and Ports” is a European project that has been carried out since 2009 to handle wind forecast in port areas through an integrated system made up of an extensive in-situ wind monitoring network, the numerical simulation of wind fields, the statistical analysis of wind climate, and algorithms for medium-term (1-3 days) and short term (0.5-2 hours) wind forecasting. The in-situ wind monitoring network, currently made up of 22 ultrasonic anemometers, provides a unique opportunity for detecting high resolution thunderstorm records and studying their dominant characteristics relevant to wind engineering with special concern for wind actions on structures. In such a framework, the wind velocity of thunderstorms is firstly decomposed into the sum of a slowly-varying mean part plus a residual fluctuation dealt with as a non-stationary random process. The fluctuation, in turn, is expressed as the product of its slowly-varying standard deviation by a reduced turbulence component dealt with as a rapidly-varying stationary Gaussian random process with zero mean and unit standard deviation. The extraction of the mean part of the wind velocity is carried out through a moving average filter, and the effect of the moving average period on the statistical properties of the decomposed signals is evaluated. Among other aspects, special attention is given to the thunderstorm duration, the turbulence intensity, the power spectral density and the integral length scale. Some noteworthy wind velocity ratios that play a crucial role in the thunderstorm loading and response of structures are also analyzed.

Keywords: gust factor; monitoring network; moving average period; synoptic event; thunderstorm; turbulence; wind velocity

1. Introduction

The study of thunderstorms and their actions on structures has been a dominant topic of the research in wind engineering over the last 30 years (e.g., Solari 2014). This depends firstly on the fact that the methods currently applied to determine the wind actions on structures are still referred to the synoptic-scale extra-tropical cyclones that strike mid-latitude areas; these phenomena occur

^{*}Corresponding author, Professor, E-mail: giovanni.solari@unige.it

^a Assistant Professor, E-mail: massimiliano.burlando@unige.it

^b Post-Doc Scientist, E-mail: patrizia.degaetano@unige.it

^c Associate Professor, E-mail: repetto@dicca.unige.it

in neutral atmospheric conditions with stationary features and velocity profiles in equilibrium with the planetary boundary layer (PBL). Thunderstorms are non-stationary phenomena at the meso-scale that occur in convective conditions with “nose” velocity profiles completely different from those that are typical of the PBL. Design wind velocities with mean return periods greater than 10-20 years are often associated with thunderstorms. They are in fact the dominant wind type for structural design in many parts of the world.

The literature has many contributions that describe measurements of thunderstorms elaborated to obtain the parameters of major interest for evaluating their actions on structures. Choi (2000), Choi and Hidayat (2002a), and Choi (2004) illustrated the results of a monitoring programme carried out in Singapore, giving relevance to the definition and values assumed by the gust factor. Duranona *et al.* (2006) analyzed the evolution of the vertical profile of the mean wind velocity and the turbulence properties of non-stationary events registered in north European coastal areas. Orwig and Schroeder (2007) investigated the space-time properties of the rear-flank downdraft of a super-cell and a derecho detected during a thunderstorm outflow experiment conducted in 2002 in Lubbock, Texas. Holmes *et al.* (2008) studied the rear-flank downdraft previously examined by Orwig and Schroeder (2007), decomposing its velocity into a deterministic running mean and a random turbulence component whose characteristics were inspected and discussed in detail. Gunter and Schroeder (2013) illustrated a novel project carried out at Texas Tech University aiming to perform high-resolution full-scale measures of thunderstorm outflows by using surface instruments and mobile Doppler radars. Lombardo *et al.* (2014) investigated some thunderstorms that occurred in Lubbock to elucidate their main properties relevant to wind engineering.

In spite of this impressive amount of measurements and elaborations, the understanding and representation of thunderstorms are still full of uncertainties and problems to be clarified. This depends, on the one hand, on the complexity of these phenomena and, on the other hand, on their short duration and small size. The first aspect makes it difficult to formulate models that are physically realistic and simply applicable as in the case of synoptic events. The second aspect makes still very limited the available data, and points out the necessity of collecting and investigating as many thunderstorm records as it is possible.

The project “Wind and Ports” (Solari *et al.* 2012) may offer an important contribution to the growth and advance in the knowledge of thunderstorms and their parameters relevant to wind engineering. Started in 2009 and finished in 2012, this project was financed by the European Territorial Cooperation Objective, Cross-border program “Italy-France Maritime 2007-2013”. It involved the port authorities of the five main ports in the Northern Tyrrhenian Sea, namely Genoa, La Spezia, Livorno, Savona (Italy) and Bastia (France). The Department of Civil, Chemical and Environmental Engineering (DICCA) of the University of Genoa was the only scientific partner. The project focused on the wind forecast in port areas and developed an integrated system made up of an extensive in-situ monitoring network, the numerical simulation of wind fields, the statistical analysis of wind climate, and algorithms for medium term (1-3 days) and short-term (0.5-2 hours) wind forecast. Results are made available to port operators through an integrated web-based GIS system for the safe management of port areas. The continuation of this activity after 2012 is codified by an agreement between the University of Genoa and the port authorities involved in the above project. A new European project with the same partners, “Wind, Ports and Sea”, is currently financed with the aim of continuing and developing the previous project (Burlando *et al.* 2015).

This paper analyses a first block of the data recorded during the project “Wind and Ports”, with the aim of extracting high resolution thunderstorm records and studying their dominant properties

relevant to wind engineering. Of course, such properties cannot be representative of the many types of meteorological conditions that can occur in a variety of latitudes and climate zones. However, their study may enrich the knowledge of thunderstorms, provide methodological issues on their analysis, stimulate discussion on how to improve the statistical analysis of their characteristics.

Section 2 describes the monitoring network and the dataset of the project, discussing the methods applied in order to extract thunderstorm records. Section 3 illustrates the decomposition of the wind velocity of thunderstorms into the sum of a slowly-varying mean part plus a residual fluctuation dealt with as a non-stationary random process; the fluctuation, in turn, is expressed as the product of its slowly-varying standard deviation by a reduced turbulence component dealt with as a rapidly-varying stationary Gaussian random process with zero mean and unit standard deviation; the extraction of the mean part of the wind velocity is carried out through a moving average filter. Section 4 discusses the effects of the choice of the moving average period on the statistical properties of the decomposed signals; particular attention is given to the separation of the harmonic content of the mean part and the fluctuations, and the statistical moments of the reduced turbulence. Section 5 provides a comprehensive picture of the slowly-varying mean wind velocity of thunderstorms, focusing on the critical issue of their duration. Section 6 discusses the parameterization of the turbulence intensity with special regard to the roughness of the terrain that surrounds the anemometers; the results are compared with those obtained for synoptic events. Section 7 examines the power spectral density (PSD) and the integral length scale of the reduced turbulence; also in this case the results are compared with those obtained for synoptic events. Section 8 analyses some wind velocity ratios that play a key role in the thunderstorm loading and response of structures. Section 9 summarizes the main conclusions and draws some prospects for future research on this topic.

2. Monitoring network and dataset

Fig. 1 shows the monitoring network realized for the project “Wind and Ports” (Solari *et al.* 2012). The network consists of 22 ultrasonic anemometers (circles) distributed in the Ports of Genoa (2), Savona (6), La Spezia (4), Livorno (5) and Bastia (5). The Port of Vado is adjacent to the Port of Savona and is managed by the same Port Authority; so, the Port of Savona includes the port area of Vado. Table 1 shows the main properties of these anemometers, h being their height above ground. In addition to these initial instruments, 11 ultrasonic anemometers have been installed in the Ports of Genoa (9), Savona (1) and La Spezia (1) by local port authorities (squares in Figure 1). Furthermore, in the framework of the new project “Wind, Ports and Sea” (Burlando *et al.* 2015), 6 ultrasonic anemometers are being installed in the Ports of Genoa (1), Savona (1), Livorno (2) and Ile-Rousse (2); 3 LiDARs are being installed in the Ports of Genoa (1), Savona (1) and Livorno (1). It is expected that a monitoring network made up of 39 ultrasonic anemometers and 3 LiDARs will be operational by mid-2015; thermometers, barometers and hygrometers are being also added to the anemometric network.

The position of the instruments has been chosen in order to cover homogeneously the port areas and register undisturbed wind velocity records. Instruments are mounted on high-rise towers and some antenna masts at the top of buildings, at least at 10 m height above ground level, with special attention to avoid any local effect that could contaminate signals. The sampling rate of the anemometers is 10 Hz, with the exception of the anemometers in the Port of Bastia, whose

sampling rate is 2 Hz. Wind measurements are collected with a precision of 0.01 m/s and 1 degree for wind speed and direction, respectively.

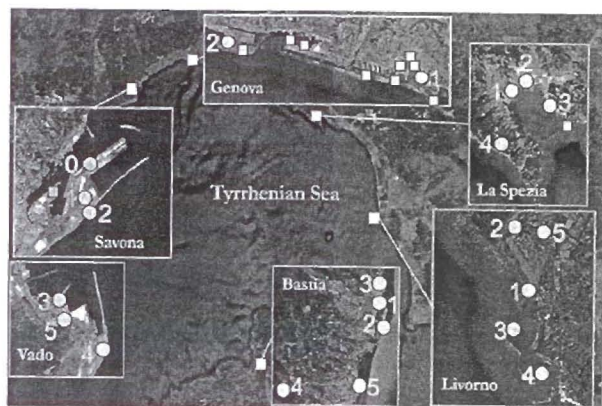


Fig. 1 Anemometric monitoring network (circles represent the anemometers installed for the project “Wind and Ports”; squares represent new anemometers)

Table 1 Main properties of the initial monitoring network

Port	Anemometer No.	h (m)	Type	Sampling rate (Hz)
Savona and Vado	0	84	tri-axial	10
	1	33		
	2	18		
	3	27		
	4	32		
Genoa	1	61,4	bi-axial	10
	2	13,3		
	3	10		
	4	11		
	5	75		
La Spezia	1	15,5	bi-axial	10
	2	13		
	3	10		
	4	11		
	5	75		
Livorno	1	20	tri-axial	10
	2	20		
	3	20		
	4	20		
	5	75		
Bastia	1	10	bi-axial	2
	2	10		
	3	13		
	4	10		
	5	10		

A set of local servers placed in each port authority headquarter receives the measurements from the anemometers in their own port area and generates basic statistics on 10-minute periods, i.e., the mean and peak wind velocities and the mean wind direction. Each server automatically sends this information to a central server in DICCA. Two files are transferred every 10 minutes containing, for each anemometer, the raw data and the statistical values of the previous 10-minute period. The operational centre of DICCA stores this data into its central dataset after having systematically checked and validated the data received. Real-time transfer is crucial for short-term forecasting (Burlando *et al.* 2014). Validation is carried out in two stages: in the first stage, carried out in real-time, the data is marked with a reliability index depending on the number of measures actually acquired in the previous 10-minute period; in the second stage, carried out periodically, the mean and peak values, the standard deviation, the skewness, the kurtosis and the harmonic content of the wind velocity are examined and compared with other simultaneous contiguous measures.

A semi-automated procedure has been implemented in order to extract and separate different intense wind events (De Gaetano *et al.* 2013). Table 2 provides the number of records examined in the present paper. They comprise 64 thunderstorm events (NTE) and 93 thunderstorm records (NTR); the 1-s peak wind velocity of all these records exceeds 15 m/s; there are more NTR than NTE because, during thunderstorm events, thunderstorm records are often registered by two or more anemometers in the same port. In addition, 97 synoptic events (NSE) and 229 synoptic records (NSR) are analysed for comparison purposes; the mean wind velocity over 10 minutes of all these records exceeds 10 m/s (nearly neutral conditions); the size of synoptic events makes NSR much larger than NSE; the sum of NSE in each port is less than NSE in all ports since the same synoptic event may be detected in different ports. The data are generated by 9 of 22 anemometers in the period 2011-2012: Anemometer 1 of the Port of La Spezia is not included in Table 2 since it provided data not fully reliable; Anemometer 4 of the Port of La Spezia and all the anemometers of the ports of Savona and Bastia started measurements later and their data have not yet been analyzed.

Table 2 Number of thunderstorm and synoptic events and records examined

Port	Anemometer No.	NTE	NTR	NSE	NSR
Genoa	1	21	12	26	18
	2		11		27
La Spezia	1	16	8	10	4
	2		14		9
Livorno	1	27	12	77	24
	2		7		28
	3		12		46
	4		5		31
	5		12		42
All ports	-	64	93	97	229

Table 3 Classes of membership of the peak wind velocity of thunderstorms

\hat{v} (m/s)	15-20	20-25	25-30	30-35
NTR	59	27	5	2

Table 3 shows the 1-s peak wind velocity values, \hat{v} , recorded during thunderstorms, divided into classes of membership. Fig. 2 shows two intense thunderstorm records registered in the Port of La Spezia: horizontal solid lines denote mean wind velocities over 1-hour periods; horizontal dotted lines correspond to mean wind velocities over 10-minute subsequent periods; circles indicate 1-s peaks (smaller than maximum wind velocities acquired with sampling rate 10 Hz). Fig. 3 shows the distribution of the thunderstorm records in Table 2 with reference to the day of occurrence (1 relates to January 1) and the wind direction in the Ports of Genoa (a), La Spezia (b) and Livorno (c). Examining together Figs. 1 and 3, it is worth noting that thunderstorms mainly occurred in the months between September and January. In the Ports of Genoa (Fig. 3(a)) and Livorno (Fig. 3(c)) most of these events come from the sea; in the Port of La Spezia (Fig. 3(b)) this is not so evident and most of the thunderstorms come from the sector between South-East and South-West.

The choice to examine all records with \hat{v} values greater than 15 m/s, adopted in the present paper, is consistent with thunderstorm analyses carried out by other authors (Choi 2000, 2004, Duranona *et al.* 2006), and with the tradition of evaluating the parameters of synoptic events by collecting all records that satisfy the requirement of neutral atmospheric conditions (Solari and Piccardo 2001, Solari and Tubino 2002), these including several phenomena of limited engineering interest. The alternative approach of restricting analyses to thunderstorms with higher \hat{v} values (Geerts 2001, Lombardo *et al.* 2014) improves the information related to those phenomena of major engineering interest, but reduces the statistical representativeness of results. Studies are in progress to extend the analyses carried out in this paper to all the thunderstorm records not yet examined (about 75% of the data currently detected by the "Wind and Ports" monitoring network), in order to inspect, based on a larger dataset, the dependence of thunderstorm parameters on the wind velocity.

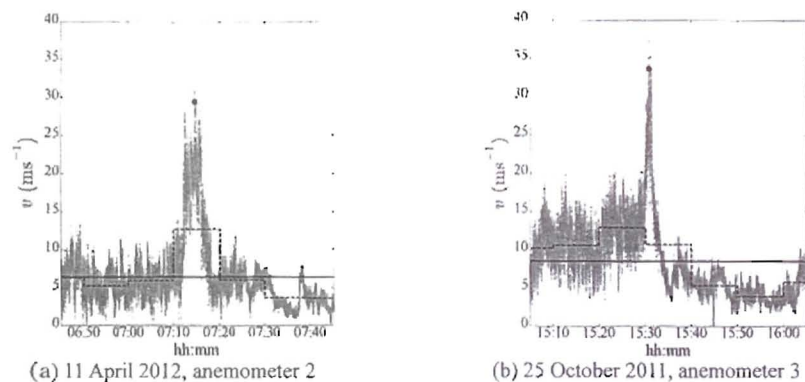


Fig. 2 Thunderstorm records registered in the Port of La Spezia

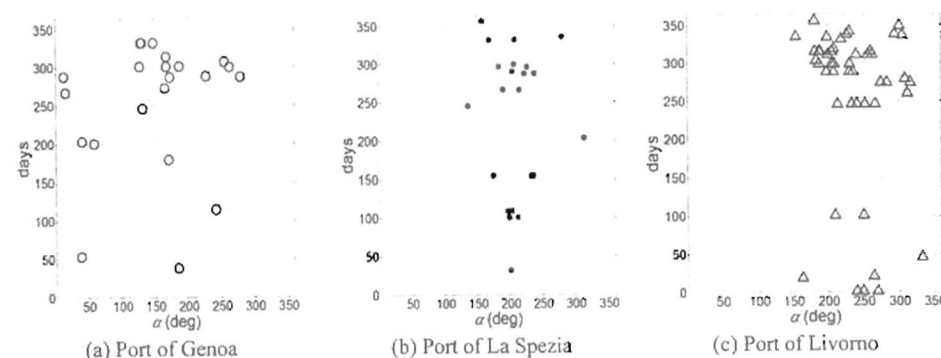


Fig. 3 Day of the year and direction of occurrence of thunderstorms

3. Wind velocity decomposition

The wind velocity in thunderstorms is usually expressed by the relationship (Choi and Hidayat 2002b, Chen and Letchford 2004)

$$v(t) = \bar{v}(t) + v'(t) \quad (1)$$

where t is the time, \bar{v} is the slowly-varying mean wind velocity, related to the low frequency content of v , v' is the residual fluctuation, related to the high frequency content of v . The extraction of \bar{v} from v may be carried out by wavelet and Hilbert transforms, empirical mode decomposition (Chen and Letchford 2007, McCullough *et al.* 2014) or, more classically as in this paper, by a moving average filter or running-mean (Choi and Hidayat 2002b, Holmes *et al.* 2008). A wide literature exists on the most suitable choice of the moving average period T : Choi and Hidayat (2002b) investigated the values $T = 10$ -120 s, suggesting that $T = 60$ s is a suitable choice; Chen and Letchford (2005, 2006) recommended $T = 32$ s; Holmes *et al.* (2008) inspected the values $T = 10, 40$ and 60 s, suggesting $T = 40$ s; Riera and Ponte (2012) used $T = 30$ s; Lombardo *et al.* (2014) adopted $T = 17$ and 34 s. A variable-interval time-averaging approach was proposed by McCullough *et al.* (2014). In this paper, an over-bar denotes a temporal average.

The mean velocity is driven by the large scale flow and is often modelled as deterministic; the fluctuating velocity is induced by the small scale turbulence and may be dealt with as a non-stationary random process given by

$$v'(t) = \sigma_v(t) \tilde{v}'(t) \quad (2)$$

where σ_v is the slowly-varying standard deviation of v' , \tilde{v}' is referred to as the reduced turbulent fluctuation and is usually dealt with as a rapidly-varying stationary Gaussian random process with zero mean and unit standard deviation (Chen and Letchford 2004).

The slowly-varying standard deviation σ_v is conceptually of medium scale (Chen and Letchford 2004): on the one hand, it is a property of the fluctuation at the turbulence scale; on the other hand, it is driven by the mean wind velocity at the large scale and is thus often modelled as deterministic.

The reduced turbulent fluctuation \tilde{v}' , linked with the atmospheric turbulence, is of a small scale. There is a wide literature on the properties of \tilde{v}' , with special concern for the analogies between its harmonic content and that of stationary synoptic events (Chen and Letchford 2004, 2005, Holmes *et al.* 2008, Kwon and Kareem 2009, Lombardo *et al.* 2014).

Combining Eq. (2) with Eq. (1), the wind velocity v may be rewritten as

$$v(t) = \bar{v}(t)[1 + I_v(t)\tilde{v}'(t)] \quad (3)$$

where I_v is referred to as the time-varying turbulence intensity

$$I_v(t) = \frac{\sigma_v(t)}{\bar{v}(t)} \quad (4)$$

Likewise \bar{v} and σ_v , also I_v depends on the moving average period T . In addition, since I_v is generally a weakly-dependent function of time, it is rather usual to identify this quantity through its average value \bar{I}_v over a suitable averaging time period (Section 6).

The above wind velocity decomposition coincides with the classical one, usually adopted for stationary synoptic events, provided that \bar{v} and σ_v are, respectively, the mean value and the standard deviation referred to an averaging time period T in the order of 10 minutes.

4. Moving average period

The choice of the moving average period T should be a compromise between two opposite tendencies: if T is too large, the residual fluctuation contains proper elements of the large scale wind structure; if T is too small, the time-varying mean part of the velocity involves turbulence fluctuations at the small scale. Figs. 4-7 show the wind velocity decomposition of the thunderstorm recorded by the anemometer 3 of the Port of La Spezia on 24 December 2011; the record length is 10 minutes; the moving average period is $T = 10, 20, 30$ and 40 s, respectively. Panels (a)-(f) report, respectively, $v, \bar{v}, v', \sigma_v, I_v$ and \tilde{v}' ; panel (a) is the same in the four figures. Fig. 4 shows that, for $T = 10$ s, the time-varying mean part of the velocity involves some fluctuations at the small scale, while the residual fluctuation is almost totally lacking of any trend associated with the large scale wind structure. Fig. 7 shows that, for $T = 40$ s, the time-varying mean part of the velocity does not contain any fluctuation at the small scale, but the residual fluctuation exhibits apparent elements of the large scale wind structure. Figs. 5 and 6, related to $T = 20$ s and $T = 30$ s, respectively, show intermediate properties according to which the time-varying mean part of the velocity involves limited fluctuations at the small scale, while the residual fluctuation exhibits limited elements of the large scale wind structure.

In order to elucidate this concept from a different viewpoint, it is worth noting that in the case of stationary synoptic events, the spectral gap separates the frequency content of the mean and fluctuating parts of the velocity. It is advisable that the time-varying mean part and the residual fluctuation have distinct frequency contents also in the case of non-stationary thunderstorms. Fig. 8 depicts the separation between the low frequency content of the time-varying mean part of the wind velocity \bar{v} and the high frequency content of the residual fluctuation v' related to the thunderstorm decompositions in Figs. 4-7.

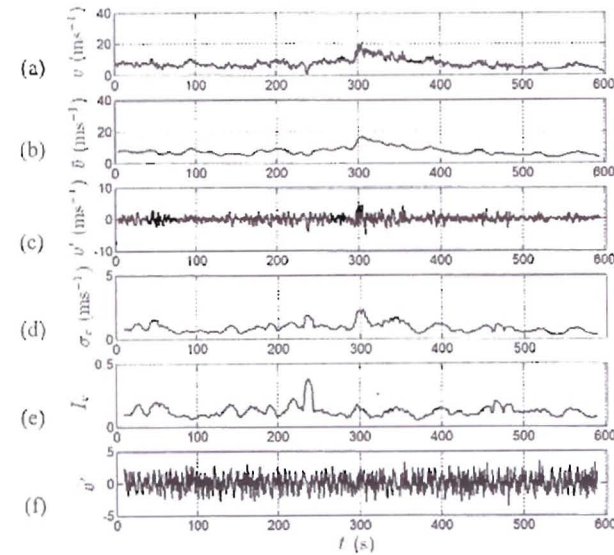


Fig. 4 Wind velocity decomposition of a thunderstorm record for $T = 10$ s: (a) v ; (b) \bar{v} ; (c) v' ; (d) σ_v ; (e) I_v ; (f) \tilde{v}'

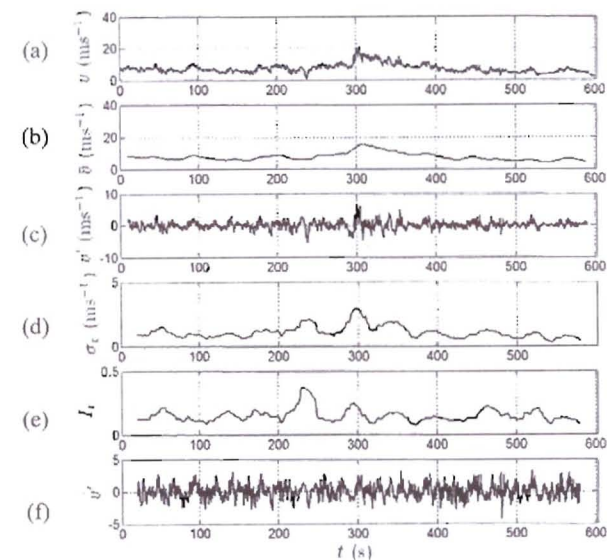


Fig. 5 Wind velocity decomposition of a thunderstorm record for $T = 20$ s: (a) v ; (b) \bar{v} ; (c) v' ; (d) σ_v ; (e) I_v ; (f) \tilde{v}'

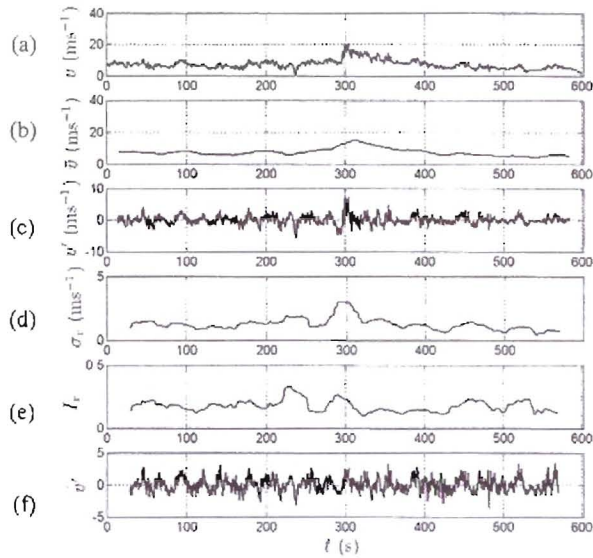


Fig. 6 Wind velocity decomposition of a thunderstorm record for $T = 30$ s: (a) v ; (b) \bar{v} ; (c) v' ; (d) σ_v ; (e) I_r ; (f) \bar{v}'

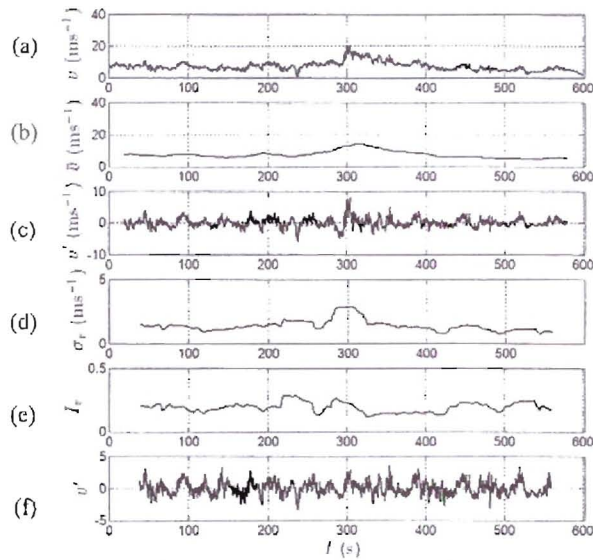


Fig. 7 Wind velocity decomposition of a thunderstorm record for $T = 40$ s: (a) v ; (b) \bar{v} ; (c) v' ; (d) σ_v ; (e) I_r ; (f) \bar{v}'

Panels (a)-(d) correspond to $T = 10, 20, 30$ and 40 s, respectively. Each panel shows the diagrams of the functions $n|F_{\bar{v}}|^2$, $n|F_{v'}|^2$, and $n|F_{\bar{v}}||F_{v'}|$, where n is the frequency; $F_{\bar{v}}$ and $F_{v'}$ are the Fourier transforms of \bar{v} and v' , respectively, scaled by the 1-s peak \hat{v} . If the frequency contents of \bar{v} and v' were totally disjoint, $n|F_{\bar{v}}||F_{v'}| = 0$. Let us define the quantity

$$J = \int_{-\infty}^{\infty} n|F_{\bar{v}}(n)||F_{v'}(n)|dn \quad (5)$$

Eq. (5) provides a compact measure of how much the frequency contents of \bar{v} and v' are disjoint; of course, J depends on T . For J tending to zero, the running mean separates the frequency contents of \bar{v} and v' . On increasing J , the frequency contents of \bar{v} and v' tend to overlap. Table 4 shows the mean value and the standard deviation (std) of J , as functions of T (in the range $T = 5-60$ s), for all the thunderstorm records detected in the ports of Genoa, La Spezia and Livorno. J approaches its minimum value for $T = 30-40$ s; the std value of J is almost independent of T .

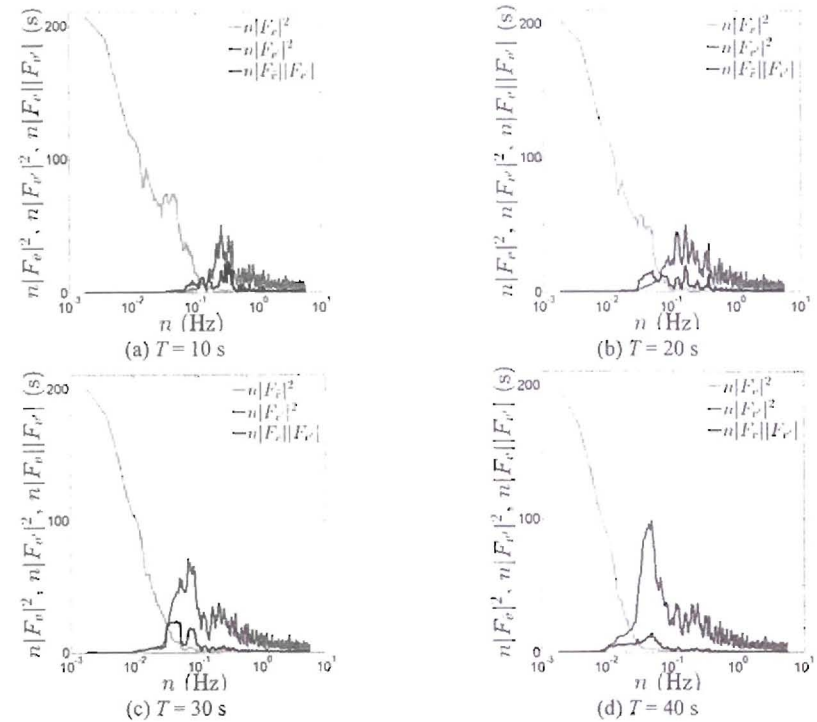


Fig. 8 Functions $n|F_{\bar{v}}|^2$, $n|F_{v'}|^2$ and $n|F_{\bar{v}}||F_{v'}|$ associated with a thunderstorm record

Table 4 Mean and std values of J , for all the thunderstorm records

T (s)	5	10	20	30	40	60
Mean(J)	4.75	4.49	4.31	4.21	4.20	4.28
Std(J)	2.82	2.90	2.96	2.91	2.96	2.93

Table 5 Mean and std values of $\mu_{\tilde{v}'} / \tilde{v}'$, for all the thunderstorm records

T (s)	5	10	20	30	40	60
Mean($\mu_{\tilde{v}'} / \tilde{v}'$)	0.000	0.000	0.000	0.000	0.000	0.000
Std($\mu_{\tilde{v}'} / \tilde{v}'$)	0.000	0.001	0.001	0.002	0.003	0.002

It is also suitable that the residual fluctuation v' has an almost zero mean value, i.e., $\mu_{v'} \approx 0$. Table 5 shows the mean and std values of $\mu_{v'}$ scaled by the 1-s peak \tilde{v}' of v' , as functions of T , for all the thunderstorm records detected. As recommended, the mean value of $\mu_{v'} / \tilde{v}'$ is very close to zero for any T ; its std value slightly increases with increasing T .

Finally, since the reduced turbulent fluctuation \tilde{v}' is usually dealt with as a stationary Gaussian random process with zero mean and unit standard deviation, it is advisable that the running mean has mean value $\mu_{\tilde{v}'} \approx 0$, standard deviation $\sigma_{\tilde{v}'} \approx 1$, skewness $\gamma_{\tilde{v}'} \approx 0$ and kurtosis $\kappa_{\tilde{v}'} \approx 3$. Table 6 shows the mean and std values of $\mu_{\tilde{v}'}$, $\sigma_{\tilde{v}'}$, $\gamma_{\tilde{v}'}$ and $\kappa_{\tilde{v}'}$, as functions of T , for all the thunderstorm records detected. The above conditions are on average well satisfied for any T , with a moderate exception for the skewness, which is on average $\gamma_{\tilde{v}'} \approx 0.1$, and the kurtosis, which is on average $\kappa_{\tilde{v}'} \approx 2.8$. The std values of all the above parameters increase on increasing T .

Based on all these remarks, and taking into account the suggestions of other authors, $T = 30$ s seems to be a reasonable choice. The following analyses adopt this moving average period.

Fig. 9 shows the probability density function (PDF) of \tilde{v}' for all the 93 thunderstorm records detected, compared with the Gaussian PDF. The slight detachment from the target curve quantifies the consequence of a skewness moderately lower than 0 and a kurtosis moderately lower than 3.

Table 6 Mean and rms values of $\mu_{\tilde{v}'}$, $\sigma_{\tilde{v}'}$, $\gamma_{\tilde{v}'}$ and $\kappa_{\tilde{v}'}$, for all the thunderstorm records

T (s)	5	10	20	30	40	60
Mean($\mu_{\tilde{v}'}$)	0.005	0.001	-0.003	-0.005	-0.008	-0.010
Std($\mu_{\tilde{v}'}$)	0.006	0.008	0.013	0.019	0.021	0.028
Mean($\sigma_{\tilde{v}'}$)	1.002	1.003	1.003	1.004	1.005	1.007
Std($\sigma_{\tilde{v}'}$)	0.005	0.007	0.008	0.010	0.012	0.015
Mean($\gamma_{\tilde{v}'}$)	-0.046	-0.074	-0.091	-0.096	-0.097	-0.070
Std($\gamma_{\tilde{v}'}$)	0.060	0.083	0.111	0.137	0.156	0.181
Mean($\kappa_{\tilde{v}'}$)	2.758	2.790	2.822	2.834	2.844	2.854
Std($\kappa_{\tilde{v}'}$)	0.139	0.182	0.223	0.222	0.243	0.253

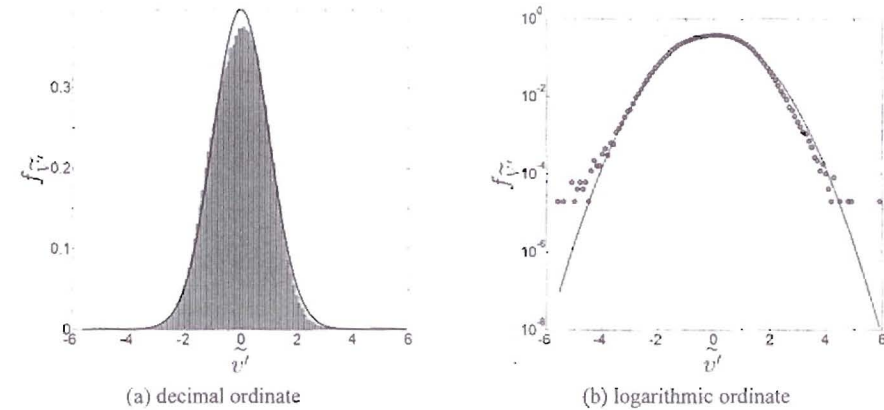


Fig. 9 PDF of the reduced turbulent fluctuations

5. Thunderstorm duration

One of the most debated aspects in literature is the time period during which thunderstorms develop their own maximum intensity. The Andrews AFB downdraft had a ramp-up period of about 90-100 s (Fujita 1990); following Choi and Hidayat (2002a) and Kwon and Kareem (2009), high thunderstorm wind velocities last around 120-180 s; Duranona *et al.* (2007) found that the wind velocity increases from 120 to 360 s, and decreases in about 90-480 s; Holmes *et al.* (2008) noted that high amplitude wind velocities occur in approximately 100 s; Lombardo *et al.* (2014) suggested that a suitable time period for evaluating thunderstorm parameters is around 60-240 s. Analytical laws and discussions aiming to describe the shape of the speed rise-decay were provided for instance by Holmes and Oliver (2000), Kwon and Kareem (2009), and Abd-Elaal *et al.* (2014).

Let us introduce the non-dimensional function

$$\gamma(t) = \frac{\bar{v}(t)}{\bar{v}_{max}} \quad (6)$$

where \bar{v}_{max} is the maximum value of the slowly-varying mean velocity \bar{v} .

Fig. 10(a) shows a typical diagram of γ ; the abscissa is shifted so that \bar{v}_{max} occurs at $t = 0$. $T_i = -t_i$ and $T_d = t_d$ are referred to as the thunderstorm increasing (ramp-up) and decreasing time period, respectively, t_i and t_d being the conventional values of t for which the most intense part of the thunderstorm begins and finishes; $T_t = T_i + T_d$ is referred to as the total duration of the most intense part of the thunderstorm; $\gamma = 0.6$ corresponds to a wind velocity pressure equal to 36 % of its maximum value. Fig. 10(b) shows the ensemble of the diagrams of γ for all the thunderstorm records detected; the thick line corresponds to the mean value of γ as a function of time. Table 7 shows the mean value, the coefficient of variation (cov) and the minimum value of T_i , T_d and T_t for all the thunderstorm records detected by each anemometer and the whole monitoring network.

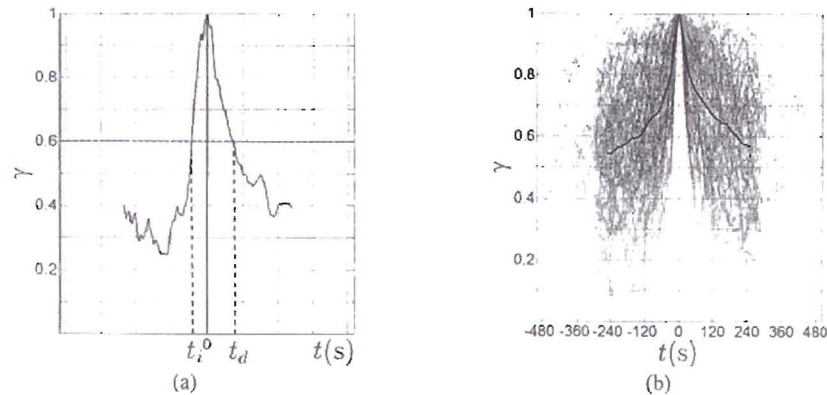


Fig. 10 (a) Typical diagram of γ for a thunderstorm record; (b) ensemble of the diagrams of γ for all the thunderstorm records investigated and their mean value (thick line)

Table 7 Mean values, covs and minimum values of T_b , T_d and T_i for all the thunderstorm records

Port	Anem. No.	Mean(T_i) (s)	Cov(T_i) (s)	Min(T_i) (s)	Mean(T_d) (s)	Cov(T_d) (s)	Min(T_d) (s)	Mean(T_b) (s)	Cov(T_b) (s)	Min(T_b) (s)
Genoa	1	102.9	0.70	24.2	105.4	0.71	32.3	208.3	0.69	57.0
	2	146.2	0.66	26.5	171.1	0.45	37.5	317.3	0.42	84.5
La	2	119.8	0.43	40.0	92.4	0.59	32.0	212.2	0.24	133.7
Spezia	3	105.4	0.78	26.4	98.8	0.61	26.6	204.2	0.60	64.6
Livorno	1	109.8	0.62	48.4	149.2	0.48	69.6	259.0	0.41	118.0
	2	55.6	0.44	22.1	149.8	0.69	29.5	205.4	0.48	77.3
	3	171.2	0.58	51.3	169.3	0.34	32.5	340.5	0.35	119.5
	4	185.3	0.39	127.4	195.3	0.17	150.0	380.6	0.10	277.4
	5	76.7	0.92	22.1	119.5	0.67	32.6	196.2	0.59	77.8
All ports		116.1	0.72	22.1	131.9	0.59	26.6	248.0	0.52	57.0

Fig. 10 and Table 7 show the great variability of the functions γ ; as such, they can be regarded as samples of a non-stationary process. The mean values of T_b , T_d and T_i , respectively about 116, 132 and 248 s, are rather consistent with those provided by literature. The minimum values of T_b , T_d and T_i , respectively about 22, 27 and 57 s, emphasize the possibility that some thunderstorms

involve very rapid variations of the wind velocity; on increasing the number of the available thunderstorm records, it will be interesting to investigate the correlation between the thunderstorm duration and its intensity.

Fig. 10(b) shows that the inner envelope of the diagrams of γ closely approximates the shape of the half-sine wave function used by Kwon and Kareem (2009) to model the slowly-varying mean part of the wind velocity; however, the actual trend corresponding to each different thunderstorm record is very different from the above function.

6. Turbulence intensity

As noted in Section 3, the time-varying turbulence intensity I_v , defined by Eq. (4), is usually a weakly-dependent function of time; this induced several authors to adopt thunderstorm models in which I_v is replaced by its average value \bar{I}_v over a suitable averaging time period. Referring to an averaging time period in the order of 10 minutes, Chen and Letchford (2004) initially proposed to assign $\bar{I}_v = 0.25$, then they adopted $\bar{I}_v = 0.085-0.088$ (Chen and Letchford 2007); Chay *et al.* (2006) investigated the range of the values $\bar{I}_v = 0.01-0.25$. Holmes *et al.* (2008) argued that, in proximity of the maximum value of the running mean, $\bar{I}_v = 0.09-0.11$; differently from the above estimates, this value is averaged over a period in the order of T . Literature also contains discussion on whether and how much \bar{I}_v depends on the local roughness of the terrain (Wood *et al.* 2001, Kim and Hangan 2007, Xu and Hangan 2008, Mason *et al.* 2009, Kwon and Kareem 2009, Vermeire *et al.* 2011, Orf *et al.* 2012). Lombardo *et al.* (2014) made critical remarks on some contradictory aspects reported in literature with reference to \bar{I}_v . The analysis of the turbulence intensities detected for the project "Wind and Ports" may provide some useful contributions to this discussion.

Let us introduce the non-dimensional function

$$\mu(t) = \frac{I_v(t)}{\bar{I}_v} \quad (7)$$

where \bar{I}_v is the value of I_v averaged on a 10-minute interval. Fig. 11(a) shows the ensemble of the diagrams of μ for all the thunderstorm records detected; they are extracted in such a way that the most intense wind speed occurs for $t = 300$ s; the thick line corresponds to the mean value of μ as a function of time. Fig. 11(b) shows the cov of μ as a function of time. Considering the wide variability of the diagrams of μ , it is worth noting that both their mean value and cov are nearly independent of time; this implies that each diagram of μ can be regarded as a sample function of a stationary process. It follows that, in mean terms, the average value of the turbulence intensity \bar{I}_v is nearly independent of its averaging time period.

In the literature it is usual to assign $I_v = \bar{I}_v$, based on its weak dependence on time (Figs. 4-7) and the persistent lack of data; this corresponds to assume $\mu = 1$, namely to identify μ with its mean value. This choice seems to be questionable for at least two reasons. First, as Fig. 11 shows, the set of the samples of μ denotes a sort of asymmetry with respect to the mean, typical of a non-Gaussian distribution; thus, the mean value of I_v may not represent the best choice to describe this quantity. Second, in Eq. (3) I_v multiplies \bar{v}' ; dealing with I_v as a function of time is equivalent to introduce a

modulation of \tilde{v}' usually disregarded. This matter deserves more studies especially concerning its consequences on the wind loading of structures.

Table 8 provides a comparison between the turbulence intensity of thunderstorms and synoptic events as detected by each anemometer and the whole network (Table 2). The first and second columns provide the mean value and the cov of the turbulence intensity of thunderstorms, $\bar{I}_{v,t}$. The third and fourth columns provide the same information for the turbulence intensity of synoptic events, $I_{v,s}$. As argued by Holmes *et al.* (2008) when analysing the Lubbock rear-flank downdraft of 2002, this table shows that the mean value of the average turbulence intensity of thunderstorms, $\text{mean}(\bar{I}_{v,t}) = 0.12$, is much lower than that of synoptic events, $\text{mean}(I_{v,s}) = 0.17$. The cov of the average turbulence intensity of thunderstorms, $\text{cov}(\bar{I}_{v,t}) = 0.25$, and synoptic events, $\text{cov}(I_{v,s}) = 0.23$, are similar. Other evaluations not reported here confirm that the mean value of the turbulence intensity of thunderstorms averaged over 1-minute intervals centred around the 1-s peak \hat{v} of v is almost the same of the mean value of the turbulence intensity averaged over 10-minute intervals. Of course, on decreasing the averaging time, the cov of the turbulence intensity increases.

Fig. 12 shows, for some anemometers of the wind monitoring network (Fig. 1, Table 1), the dependence of the turbulence intensity I_v (left ordinate) on the wind direction α (abscissa). The solid circles refer to the measured values of the average turbulence intensity of thunderstorms, $\bar{I}_{v,t}$; the stars refer to the measured values of the turbulence intensity of synoptic events, $I_{v,s}$. The black lines with open circles represent numerical estimates of the turbulence intensity, $I_{v,n}$, at the height $z = h$ of each anemometer; they are based on the assumption of synoptic events and neutral atmospheric conditions, and take into account the local topography and the upwind roughness features (ESDU 1993, Castino *et al.* 2003, Burlando *et al.* 2007, 2010, 2013). The grey lines with open squares represent the equivalent roughness length z_0 (right ordinate) evaluated, for each anemometer and each wind direction, by inverting the relationship:

$$I_{v,n} = \frac{1}{\ln(z/z_0)} \tag{8}$$

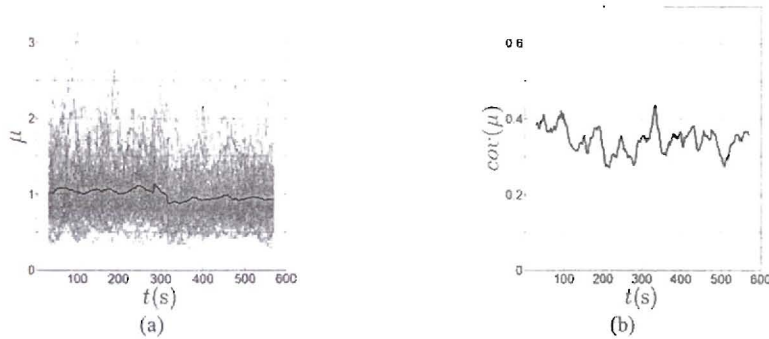


Fig. 11 (a) Ensemble of the diagrams of μ for all the thunderstorm records investigated and their mean value (thick line); (b) coefficient of variation of μ

Table 8 Mean value and cov of the turbulence intensity

Port	Anemometer No.	Thunderstorms		Synoptic events	
		Mean($\bar{I}_{v,t}$)	Cov($\bar{I}_{v,t}$)	Mean($I_{v,s}$)	Cov($I_{v,s}$)
Genoa	1	0.12	0.49	0.16	0.25
	2	0.12	0.22	0.18	0.20
La Spezia	2	0.17	0.16	0.23	0.09
	3	0.14	0.25	0.21	0.18
Livorno	1	0.10	0.41	0.16	0.34
	2	0.16	0.17	0.19	0.20
	3	0.08	0.14	0.14	0.22
	4	0.07	0.07	0.14	0.35
	5	0.13	0.35	0.17	0.28
All ports		0.12	0.25	0.17	0.23

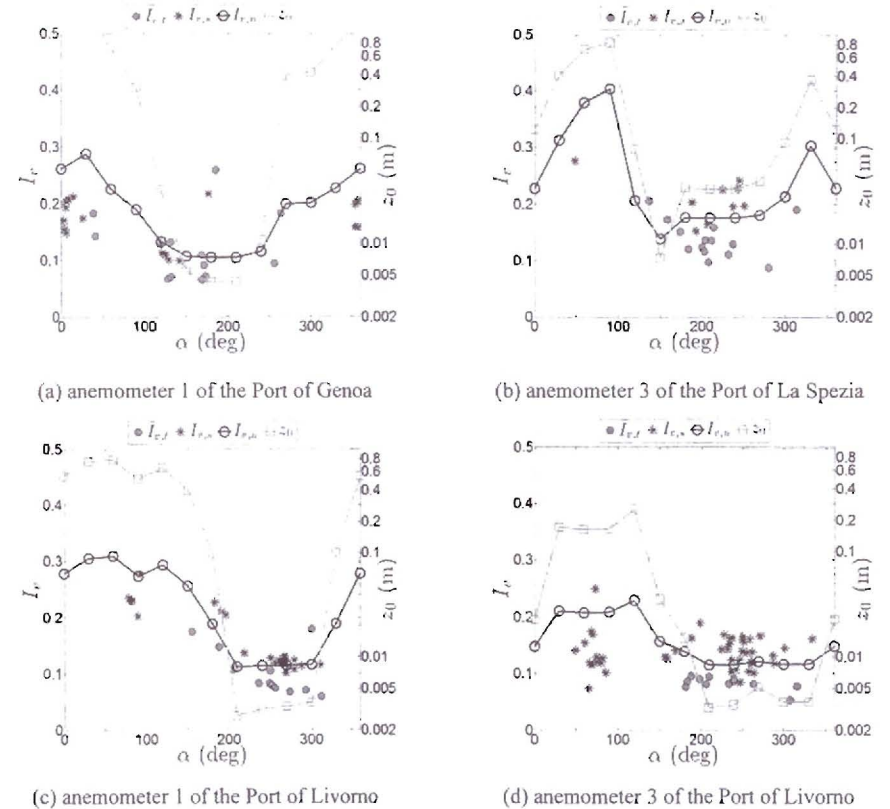
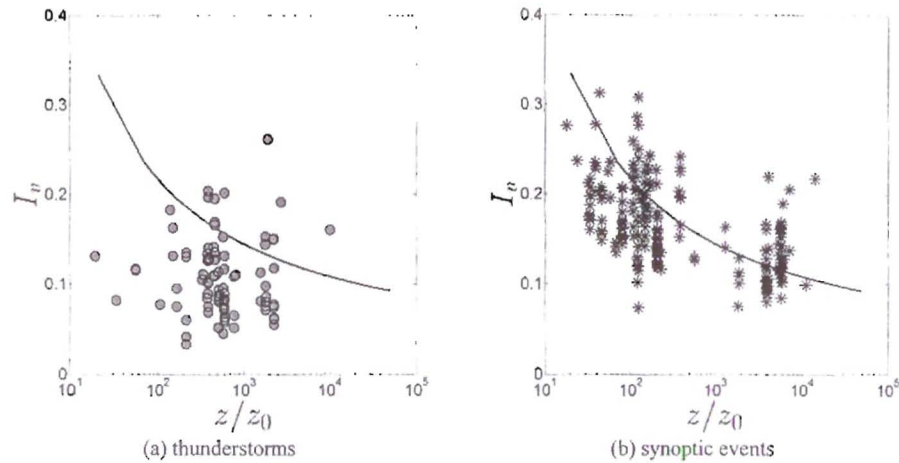


Fig. 12 Turbulence intensity and local roughness length as functions of the wind direction

Fig. 13 Turbulence intensity as a function of z/z_0

Thus, z_0 values provided by Eq. (8) strictly refer to classical neutral and synoptic wind conditions. At least on average, the measured values of the turbulence intensity of synoptic events match rather closely Eq. (8), exhibiting a regular dependence on the wind direction. The average turbulence intensity of thunderstorms does not seem to depend on the wind direction also because, for each port area, most of the available data is restricted to specific sectors (Fig. 3). In any case, as shown by Table 8, the turbulence intensity of thunderstorms is on average much lower than that of synoptic events.

Fig. 13 collects the results of the analyses into two schemes that provide the turbulence intensity of thunderstorms (a) and synoptic events (b), respectively, as a function of z/z_0 ; the solid lines correspond to Eq. (8). As far as thunderstorms are concerned, the measured turbulence intensity does not show any apparent dependence on z/z_0 . Instead, in spite of a rather large spread, synoptic events exhibit the classical trend in accordance with which the measured turbulence intensity tends to diminish on increasing z/z_0 . Also Fig. 13 shows that the turbulence intensity of thunderstorms is on average much lower than that of synoptic events.

The whole of this information points out that z/z_0 , which provides a key parameterization of the planetary boundary layer with reference to synoptic events, plays a limited role in the thunderstorm turbulence intensity and, as a consequence, in the thunderstorm wind field. This does not mean, however, that the roughness length has negligible importance. Xu and Hangan (2008) carried out wind tunnel tests that pointed out the noteworthy role of D/z_0 , D being the diameter of the impinging jet. Unfortunately, neither the measurements carried out in the framework of the project "Wind and Ports", nor other monitoring campaigns, provide enough data on the diameter of the thunderstorm downdraft.

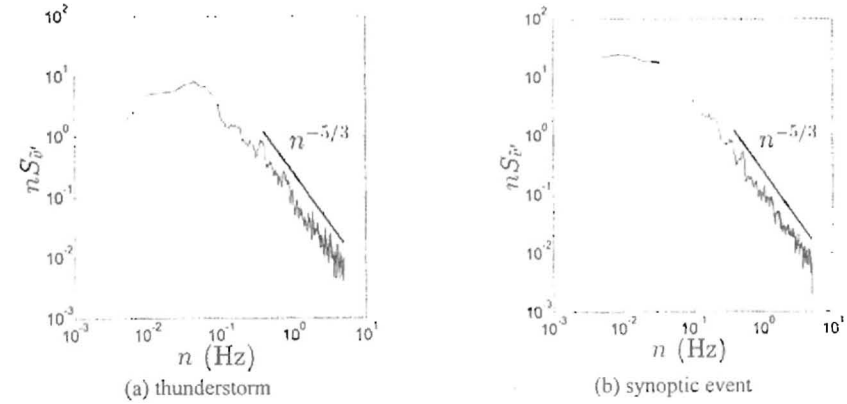


Fig. 14 PSD of the reduced turbulent fluctuation

7. Turbulence power spectral density and integral length scales

Technical literature is rather consistent in affirming that the PSD of the reduced turbulent fluctuation \tilde{v}' of thunderstorms has similar properties to the classical PSD of synoptic events (Chen and Letchford 2004, Holmes *et al.* 2008, Kwon and Kareem 2009, Lombardo *et al.* 2014). However, the discussion concerning the integral length scale of \tilde{v}' is quite controversial and very limited (Orwig and Schroeder 2007, Lombardo *et al.* 2014).

Fig. 14 shows the PSD of \tilde{v}' for a thunderstorm (a) and a synoptic event (b); each panel reports also the slope of the curve $n^{-5/3}$ related to the inertial sub-range of synoptic events (Solari 1987, Solari and Piccardo 2001). Analogous trends occur for all the thunderstorms and synoptic events detected, confirming that their PSDs have similar qualitative properties.

The integral length scale of turbulence L_v is estimated by fitting the experimental PSD of \tilde{v}' (with unit std) by the model proposed by Solari and Piccardo (2001) for stationary synoptic events

$$nS_{\tilde{v}'}(n) = \frac{f/f_m}{(1+1.5f/f_m)^{5/3}} \quad (9)$$

$S_{\tilde{v}'}$ is the PSD of \tilde{v}' ; $f = n\bar{z}/\bar{v}_{max}$ is the reduced frequency in which the mean wind velocity \bar{v} is identified with its maximum value \bar{v}_{max} (Choi and Hidayat 2002); $f_m = 0.1456z/L_v$ is the value of f for which $nS_{\tilde{v}'}$ is maximum. Fig. 15 shows the typical approximations involved by fitting the PSD of a thunderstorm (a) and a synoptic event (b).

Analogously to Table 8, Table 9 compares the integral length scale of thunderstorms and synoptic events as detected by each anemometer and the whole network. The first and second columns provide the mean value and the cov of the integral length scale of thunderstorms, $L_{v,t}$. The third and fourth columns provide the same information for the integral length scale of synoptic events, $L_{v,s}$, with mean wind velocity above 10 m/s. This table points out that the integral length scale of thunderstorms

is on average much lower than that related to synoptic events. A possible qualitative explanation of this remark may be given observing that the integral length scale of turbulence is the average size of its eddies; in a PBL flow, the maximum size of eddies is the height of the PBL. Since the outflows of thunderstorms occur in proximity of ground, both the maximum and average size of their eddies are potentially smaller than those of synoptic events. The choice of adopting a reduced frequency involving the maximum value of the mean wind velocity contributes to decrease the value of the integral length scale of thunderstorms. The cov of the integral length scale of thunderstorms is similar to that of synoptic events. Further and deeper studies are needed to confirm or clarify the above remarks.

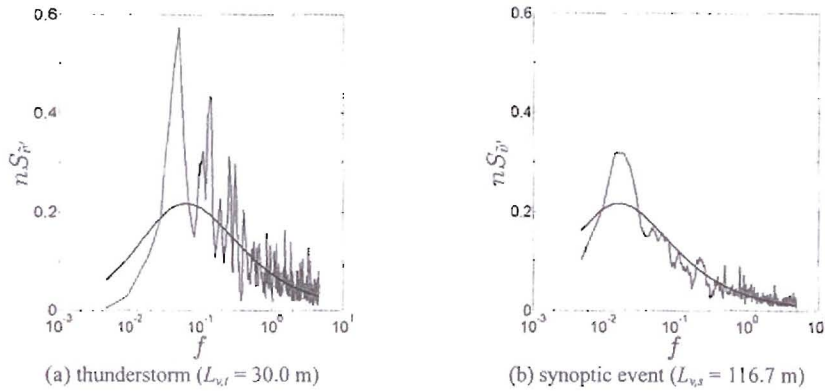


Fig. 15 Matching between the measured and theoretical PSD of the reduced turbulent fluctuation

Table 9 Mean value and cov of the integral length scale of the turbulence

Port	Anemometer No.	Thunderstorms		Synoptic events	
		Mean($L_{v,t}$) (m)	Cov($L_{v,t}$)	Mean($L_{v,s}$) (m)	Cov($L_{v,s}$)
Genoa	1	41.5	0.25	137.1	0.38
	2	35.0	0.32	94.0	0.27
La Spezia	2	32.7	0.23	161.1	0.54
	3	27.5	0.30	169.5	0.48
Livorno	1	37.7	0.43	128.6	0.29
	2	39.3	0.39	100.5	0.35
	3	33.8	0.25	125.8	0.35
	4	32.0	0.29	148.4	0.32
	5	32.6	0.42	112.9	0.29
All ports		34.6	0.34	123.1	0.38

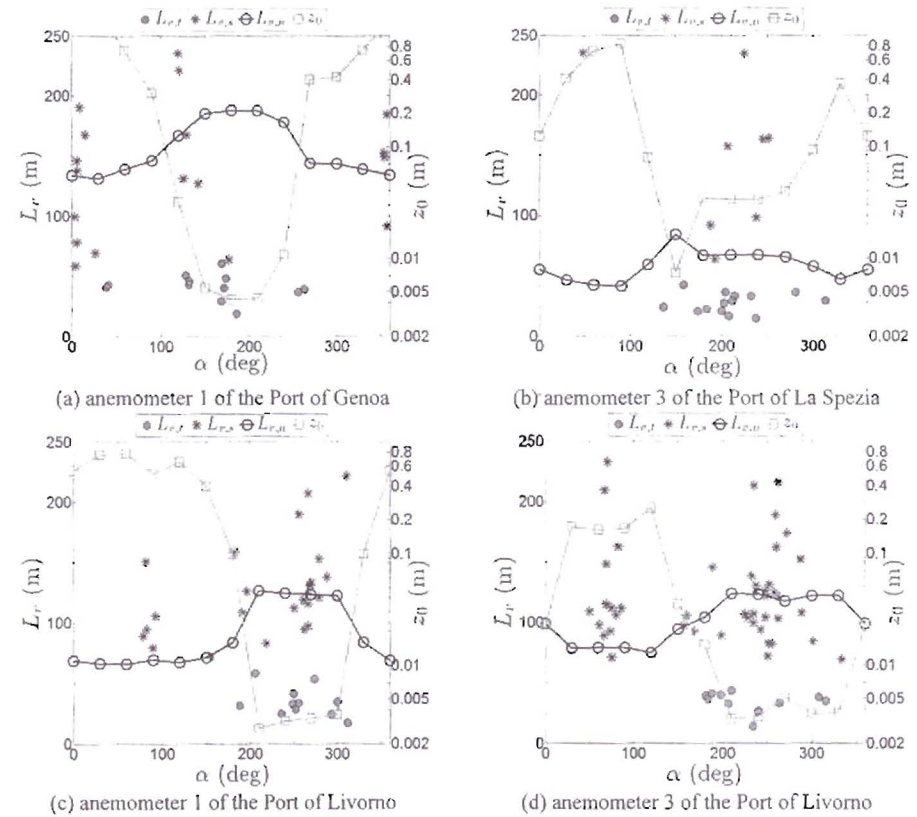


Fig. 16 Integral length scale and local roughness length as functions of the wind direction

Fig. 16 shows, for some anemometers of the wind monitoring network (Fig. 1, Table 1), the dependence of the integral length scale L_v (left ordinate) on the wind direction α (abscissa). The solid circles refer to the measured values of the integral length scale of thunderstorms, $L_{v,t}$; the stars refer to the measured values of the integral length scale of synoptic events, $L_{v,s}$. The grey lines with open squares refer to the roughness lengths z_0 (right ordinate) reported in Fig. 12. The black lines with open circles correspond to the empirical relationship for synoptic events (Solari and Piccardo 2001)

$$L_{v,s}(z) = \bar{L} \left(\frac{z}{\bar{z}} \right)^\nu \quad (z \leq \bar{L}) \quad (10)$$

where $\nu = 0.67 + 0.05 \cdot \ln(z_0)$, $\bar{L} = 300$ m, $\bar{z} = 200$ m, z_0 is expressed in meters. Even though with very large dispersion, the measured values of the integral length scale of synoptic events on average match Eq. (10). Instead, like the turbulence intensity (Fig. 12), also the integral length scale

of thunderstorms does not exhibit any relevant dependence on the wind direction. In any case, as pointed out by Table 9, it is on average much lower than that of synoptic events.

Fig. 17 collects the results of the analyses into two schemes that provide the integral length scale of thunderstorms (a) and synoptic events (b), respectively, as a function of z/z_0 . It shows that neither thunderstorms nor synoptic events exhibit any relevant correlation between L_v and z/z_0 .

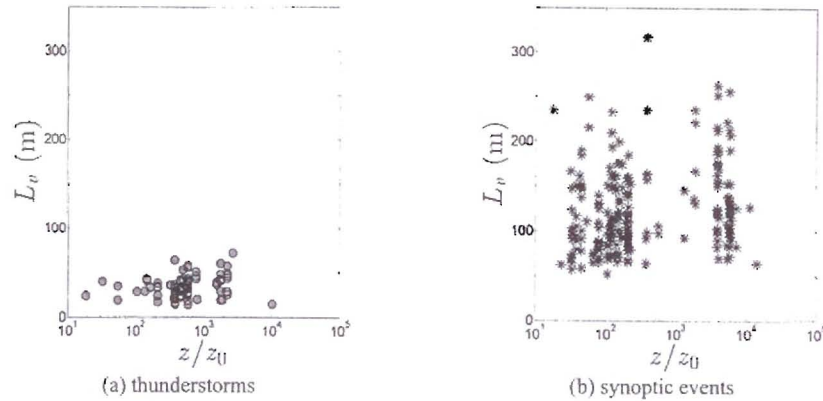


Fig. 17 Integral length scale of turbulence as a function of z/z_0

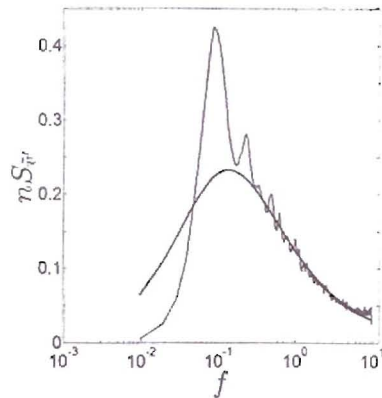


Fig. 18 Average value of the PSD of the reduced turbulent fluctuations of all the thunderstorm records detected and best fit

Based upon this remark, Fig. 18 shows the mean value of the PSD of the reduced turbulent fluctuation \bar{v}' of all the thunderstorm records detected, as a function of the reduced frequency f ; it exhibits a regular trend that closely matches Eq. (9) for $f_m = 0.055$ (thick line). In this case, the PSD of \bar{v}' assumes the form

$$nS_{\bar{v}'}(f) = \frac{18f}{(1+27f)^{5/3}} \quad (11)$$

Fig. 18 points out an excellent fit in the inertial sub-range, while it does not capture with the same precision the low frequency peak. In part, this may derive from the choice, consistent with Eq. (8), of modelling the turbulence PSD by a “blunt” model instead of a “pointed” model (Olesen *et al.* 1984, Solari and Piccardo 2001); in part this may be an inherent property of thunderstorms.

8. Noteworthy wind velocity ratios

In the case of synoptic winds, the gust factor G is referred to as the ratio between the peak wind velocity \hat{v} , averaged over a short time interval τ (in this paper $\tau = 1$ s), and the mean wind velocity \bar{V} , usually averaged over a time interval $\Delta T = 10$ ($G = G_{10}$) or 60 minutes ($G = G_{60}$)

$$G = \frac{\hat{v}}{\bar{V}} \quad (12)$$

In the case of thunderstorms, due to their non-stationary character, the value of the mean wind velocity loses meaning and Eq. (12) involves relevant peculiarities. Chay *et al.* (2008), Holmes *et al.* (2008) and Lombardo *et al.* (2014) paid great attention to the definition of a gust factor in which the mean wind velocity \bar{V} is replaced by a suitable value of the time-varying mean wind velocity \bar{v} ; since this quantity depends on the moving average period T , the gust factor of thunderstorms is in turn a function of T (Choi 2000, Choi and Hidayat 2002a, Holmes *et al.* 2008, Lombardo *et al.* 2014). Kasperski (2002) and De Gaetano *et al.* (2013) used Eq. (12) to classify and separate different types of wind events.

Generalizing the concept and the definition of the gust factor G , let us introduce three noteworthy wind velocity ratios that play a key role in the thunderstorm loading and response of structures (Solari *et al.* 2015). They are defined by the relationships

$$R = \frac{v_{max}}{\hat{v}} \quad (13)$$

$$G_{max} = \frac{v_{max}}{\bar{v}_{max}} \quad (14)$$

$$\hat{G} = \frac{\hat{v}}{\bar{v}_{max}} \quad (15)$$

where v_{max} , \hat{v} and \bar{v}_{max} are, respectively, the maximum sampled value of the wind velocity, the

1-s peak wind velocity and the maximum value of the slowly-varying mean wind velocity averaged on $T = 30$ s (Fig. 19); \hat{G} corresponds to the common definition of the gust factor of thunderstorms.

Fig. 20 provides the values assumed by R (a), G_{max} (b) and \hat{G} (c) as functions of z/z_0 for the thunderstorms detected by each anemometer of the whole network (Table 2); also these quantities do not exhibit any apparent dependence on z/z_0 . Table 10 shows the mean value and the cov of R , G_{max} and \hat{G} . The mean value of R , $\text{mean}(R) = 1.06$, is moderately greater than 1, since all the ultrasonic anemometers considered here have sampling rate 10 Hz. The mean value of G_{max} , $\text{mean}(G_{max}) = 1.27$, is approximately equal to the product of the mean values of R and \hat{G} . The mean value of \hat{G} , $\text{mean}(\hat{G}) = 1.20$, deserves some more remarks.

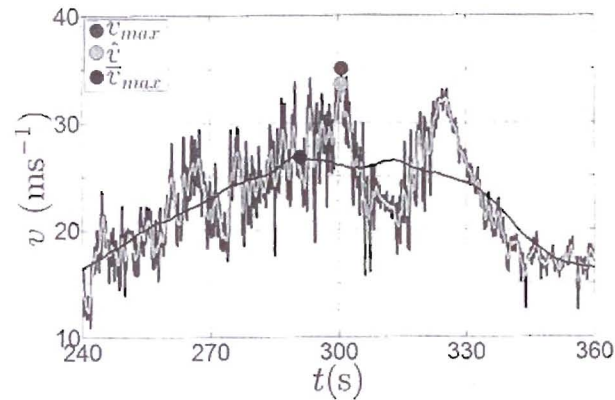


Fig. 19 Typical diagram of the wind velocity of thunderstorms: maximum value, v_{max} , 1-s peak, \hat{v} , and maximum value of the mean wind velocity averaged over $T = 30$ s, \bar{v}_{max}

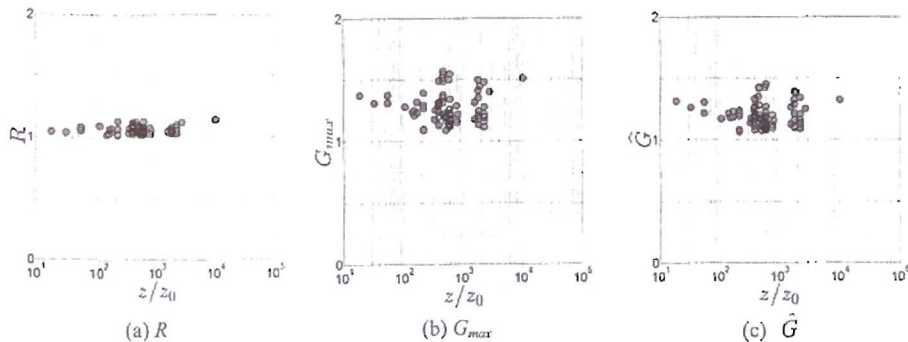


Fig. 20 Noteworthy wind velocity ratios for thunderstorms as functions of z/z_0

Table 10 Mean values and covs of three noteworthy wind velocity ratios for thunderstorms

Port	Anemometer No.	Mean(R)	Cov(R)	Mean(G_{max})	Cov(G_{max})	Mean(\hat{G})	Cov(\hat{G})
Genoa	1	1.05	0.02	1.25	0.08	1.19	0.07
	2	1.06	0.02	1.28	0.05	1.21	0.05
La	2	1.08	0.03	1.42	0.09	1.32	0.08
Spezia	3	1.06	0.03	1.30	0.09	1.22	0.07
Livorno	1	1.05	0.03	1.22	0.10	1.16	0.08
	2	1.07	0.03	1.35	0.08	1.26	0.08
	3	1.05	0.03	1.21	0.06	1.14	0.06
	4	1.04	0.02	1.15	0.04	1.11	0.04
	5	1.06	0.03	1.27	0.10	1.20	0.08
All ports		1.06	0.03	1.27	0.09	1.20	0.08

Fig. 21 provides the values assumed by G_{10} (a) and \hat{G} (b), as functions of z/z_0 , for the synoptic events detected by each anemometer of the whole network (Table 2). It is worth noting that the measured values of the classical gust factors G_{10} (Eq. (12)) exhibit a relevant dependence on z/z_0 that matches rather closely the solid lines corresponding to the analytical model developed by Solari (1993). Instead, the gust factors \hat{G} evaluated for synoptic events as it is usual for thunderstorms (Eq. (14), $T = 30$ s) seem to be almost independent of z/z_0 ; in addition, they do not follow so closely the above analytical model.

Table 11 shows a comparison between the mean value and the cov of the gust factors G_{60} , G_{10} and \hat{G} corresponding to thunderstorms and synoptic events. The comparison between the values of G_{60} and G_{10} related to thunderstorms and synoptic events shows that the former are much greater than the latter; this confirms the efficacy of using these parameters as preliminary estimators to separate the two phenomena (De Gaetano *et al.* 2013); the fact that in thunderstorms G_{60} is much greater than G_{10} confirms the results provided by De Gaetano *et al.* (2013); the fact that in synoptic events G_{60} is moderately greater than G_{10} confirms the results obtained by Solari (1983). It is worth noting that, at least for a moving average period $T = 30$ s, the mean value of \hat{G} is almost the same for thunderstorms and synoptic events. The cov always increases with increasing the gust factor.

Table 11 Mean value and cov of the gust factors

Gust factor	Thunderstorms		Synoptic events	
	Mean	Cov	Mean	Cov
G_{60}	2.58	0.33	1.63	0.14
G_{10}	1.89	0.21	1.49	0.11
\hat{G}	1.20	0.08	1.19	0.06

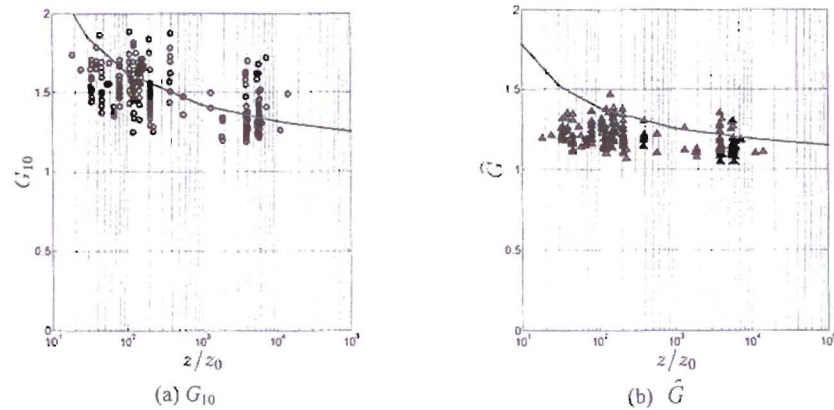


Fig. 21 Gust factors for synoptic events as functions of z/z_0

9. Conclusions

This paper deals with the main properties of thunderstorms relevant to wind engineering, with special concern for wind actions on structures. These properties are determined with reference to a preliminary set of 93 thunderstorm records detected in the Ports of Genoa, La Spezia and Livorno, in the period 2011-2012, by the monitoring network of the project "Wind and Ports".

The wind velocity of thunderstorms is expressed by means of the sum of a time-varying mean part plus a residual fluctuation. The fluctuation, in turn, is expressed as the product of its time-varying standard deviation by a reduced turbulence component. The extraction of the time-varying mean wind velocity and standard deviation is carried out by a moving average filter, or running mean, exploring the influence of the moving average period in the range $T = 5-60$ s.

The analysis shows that any $T = 20-40$ s on average provides a satisfactory separation between different flow scales and the low and high frequency content of velocity, gives rise to an almost nil mean value of the residual fluctuation, makes the reduced turbulent fluctuation actually stationary and Gaussian, except for a mean value of the kurtosis slightly less than 3. $T = 30$ s seems to represent an average and reasonable choice.

The analysis of the slowly-varying mean part of the wind velocity shows extreme variability. The mean values of the increasing, decreasing and total duration of the most intense part of the thunderstorm, T_i , T_d and T_b , are about 116, 132 and 248 s, respectively. The minimum values of T_i , T_d and T_b , respectively about 22, 27 and 57 s, points out the possibility that some thunderstorms may involve exceptionally rapid variations of the wind velocity.

The choice of identifying the time-varying turbulence intensity of thunderstorms with its mean value, frequently adopted by literature, deserves some more consideration, especially with reference to its consequences on the wind loading of structures.

The mean turbulence intensity of thunderstorms ($I_v = 0.12$) is on average much lower than that of synoptic events ($I_v = 0.17$); in addition, it does not exhibit any relevant dependence on the ratio between the height above ground and the roughness length of the terrain.

The power spectral density of the reduced turbulent fluctuation of thunderstorms shows an almost perfect similarity with that of synoptic events in the inertial sub-range. The integral length scale of the reduced turbulent fluctuation of thunderstorms ($L_v = 35$ m) is on average much lower than that of synoptic events ($L_v = 123$ m); in addition, as the turbulence intensity, it does not exhibit any relevant dependence on the ratio between the height above ground and the roughness length of the terrain.

A preliminary expression of the power spectral density of the reduced turbulent fluctuation of thunderstorms is proposed. Compared with experimental measures, it exhibits an excellent fit in the inertial sub-range, while it does not capture with the same precision the low frequency peak.

Finally, this paper reports the mean values and the coefficient of variation of three noteworthy wind velocity ratios that play a key role in the evaluation of thunderstorm actions on structures; also these quantities do not exhibit any relevant dependence on the ratio between the height above ground and the roughness length of the terrain. It is worth noting the variability of the gust factor depending on its definition and on the type of the wind event considered.

Studies are in progress to enrich analyses by a large amount of measured data not yet examined. They aim at improving and extending the statistical analysis of the characteristics of thunderstorms relevant to the wind loading of structures investigating, among other aspects, their dependence on the wind velocity.

Acknowledgments

The data exploited for this research has been recorded by the wind monitoring network of the projects "Wind and Ports" and "Wind, Port and Sea", financed by European Territorial Cooperation Objective, Cross-border program Italy-France Maritime 2007-2013. Authors thankfully acknowledge the cooperation of the Port Authorities of Genoa, La Spezia, Livorno, Savona and Bastia.

References

- Abd-Elaal, E.S., Mills, J.E. and Ma, X. (2014), "Empirical models for predicting unsteady-state downburst wind speeds", *J. Wind Eng. Ind. Aerod.*, **129**, 49-63.
- Burlando, M., Carassale, L., Georgieva, E., Ratto, C.F. and Solari, G. (2007), "A simple and efficient procedure for the numerical simulation of wind fields in complex terrain", *Bound. Lay. Meteorol.*, **125**(3), 417-439.
- Burlando, M., Freda, A., Ratto, C.F. and Solari, G. (2010), "A pilot study of the wind speed along the Rome-Naples HS/HC railway line. Part I - Numerical modelling and wind simulations", *J. Wind Eng. Ind. Aerod.*, **98**, 392-403.
- Burlando, M., De Gaetano, P., Pizzo, M., Repetto, M.P., Solari, G. and Tizzi, M. (2013), "Wind climate analysis in complex terrain", *J. Wind Eng. Ind. Aerod.*, **123**, 349-362.
- Burlando, M., Pizzo, M., Repetto, M.P., Solari, G., De Gaetano and P., Tizzi, M. (2014), "Short-term wind forecasting for the safety management of complex areas during hazardous wind events", *J. Wind Eng. Ind. Aerod.*, **135**, 170-181.

- Burlando, M., De Gaetano, P., Pizzo, M., Repetto, M.P., Solari, G. and Tizzi, M. (2015), "The European project 'Wind, Port and Seas'", *Proceedings of the 14th International Conference on Wind Engineering*, Porto Alegre, Brasil.
- Castino, F., Rusca, L. and Solari, G. (2003), "Wind climate micro-zoning: A pilot application to Liguria Region (North-Western Italy)", *J. Wind Eng. Ind. Aerod.*, **91**, 1353-1375.
- Chay, M.T., Albermani, F. and Wilson, B. (2006), "Numerical and analytical simulation of downburst wind loads", *Eng. Struct.*, **28**(2), 240-254.
- Chay, M.T., Wilson, R. and Albermani, F. (2008), "Gust occurrence in simulated non-stationary winds", *J. Wind Eng. Ind. Aerod.*, **96**(10-11), 2161-2172.
- Chen, L. and Letchford, C.W. (2004), "A deterministic-stochastic hybrid model of downbursts and its impact on a cantilevered structure", *Eng. Struct.*, **26**(5), 619-629.
- Chen, L. and Letchford, C.W. (2005), "Proper orthogonal decomposition of two vertical profiles of full-scale nonstationary correlated downburst wind speeds", *J. Wind Eng. Ind. Aerod.*, **93**(3), 187-266.
- Chen, L. and Letchford, C.W. (2006), "Multi-scale correlation analyses of two lateral profiles of full-scale downburst wind speeds", *J. Wind Eng. Ind. Aerod.*, **94**, 675-696.
- Chen, L. and Letchford, C.W. (2007), "Numerical simulation of extreme winds from thunderstorm downbursts", *J. Wind Eng. Ind. Aerod.*, **95**, 977-990.
- Choi, E.C.C. (2000), "Wind characteristics of tropical thunderstorms", *J. Wind Eng. Ind. Aerod.*, **84**, 215-226.
- Choi, E.C.C. (2004), "Field measurement and experimental study of wind speed during thunderstorms", *J. Wind Eng. Ind. Aerod.*, **92**, 275-290.
- Choi, E.C.C. and Hidayat, F.A. (2002a), "Gust factors for thunderstorm and non-thunderstorm winds", *J. Wind Eng. Ind. Aerod.*, **90**, 1683-1696.
- Choi, E.C.C. and Hidayat, F.A. (2002b), "Dynamic response of structures to thunderstorm winds", *Prog. Struct. Eng. Mat.*, **4**(4), 408-416.
- De Gaetano, P., Repetto, M.P., Repetto, T. and Solari, G. (2013), "Separation and classification of extreme wind events from anemometric data", *J. Wind Eng. Ind. Aerod.*, **126**, 132-143.
- Duranona, V., Sterling, M. and Baker, C.J. (2006), "An analysis of extreme non-synoptic winds", *J. Wind Eng. Ind. Aerod.*, **95**, 1007-1027.
- Engineering Sciences Data Unit (1993), *Computer program for wind speeds and turbulence properties: flat or hill sites in terrain with roughness changes*, ESDU Item 92032, London, U.K.
- Fujita, T.T. (1990), "Downburst: meteorological features and wind field characteristics", *J. Wind Eng. Ind. Aerod.*, **36**, 75-86.
- Geerts, B. (2001), "Estimating downburst-related maximum surface wind speeds by means of proximity soundings in New South Wales, Australia", *Weather Forecast*, **16**(2), 261-269.
- Gunter, W.S. and Schroeder, J.L. (2013), "High-resolution full-scale measurements of thunderstorm outflow winds", *Proceedings of the 12th Americas Conference on Wind Engineering*, Seattle, Washington.
- Holmes, J.D. and Oliver, S.E. (2000), "An empirical model of a downburst", *Eng. Struct.*, **22**(9), 1167-1172.
- Holmes, J.D., Hangan, H.M., Schroeder, J.L., Letchford, C.W. and Orwig, K.D. (2008), "A forensic study of the Lubbock-Reese downdraft of 2002", *Wind Struct.*, **11**(2), 19-39.
- Kasperski, M. (2002), "A new wind zone map of Germany", *J. Wind Eng. Ind. Aerod.*, **90**, 1271-1287.
- Kim, J. and Hangan, H. (2007), "Numerical simulations of impinging jets with application to downbursts", *J. Wind Eng. Ind. Aerod.*, **95**(4), 279-298.
- Kwon, D.K. and Kareem, A. (2009), "Gust-front factor: New framework for wind load effects on structures", *J. Struct. Eng.-ASCE*, **135**(6), 717-732.
- Lombardo, F.T., Smith, D.A., Schroeder, J.L. and Mehta, K.C. (2014), "Thunderstorm characteristics of importance to wind engineering", *J. Wind Eng. Ind. Aerod.*, **125**, 121-132.
- Mason, M.S., Wood, G.S. and Fletcher, D.F. (2009), "Numerical simulation of downburst winds", *J. Wind Eng. Ind. Aerod.*, **97**, 523-539.
- McCullough, M., Kwon, D.K., Kareem, A. and Wang, L. (2014), "Efficacy of averaging interval for nonstationary winds", *J. Eng. Mech.-ASCE*, **140**(1), 1-19.
- Olesen, H.R., Larsen, S.E. and Hojstrup, J. (1984), "Modelling velocity spectra in the lower part of the

- planetary boundary layer", *Bound. - Lay. Meteorol.*, **29**(3), 285-312.
- Orf, L., Kantor, E. and Savory, E. (2012), "Simulation of a downburst-producing thunderstorm using a very high-resolution three-dimensional cloud model", *J. Wind Eng. Ind. Aerod.*, **104-106**, 547-557.
- Orwig, K.D. and Schroeder, J.L. (2007), "Near-surface wind characteristics of extreme thunderstorm outflows", *J. Wind Eng. Ind. Aerod.*, **95**, 565-584.
- Riera, J.D. and Ponte, J. Jr. (2012), "Recent Brazilian research on thunderstorm winds and their effects on structural design", *Wind Struct.*, **15**(2), 111-129.
- Solari, G. (1987), "Turbulence modeling for gust loading", *J. Struct. Eng.-ASCE*, **113**(7), 1550-1569.
- Solari, G. (1993), "Gust buffeting. I: peak wind velocity and equivalent pressure", *J. Struct. Eng.-ASCE*, **119**(2), 365-382.
- Solari, G. (2014), "Emerging issues and new scenarios for wind loading on structures in mixed climates", *Wind Struct.*, **19**(3), 295-320.
- Solari, G., De Gaetano, P. and Repetto, M.P. (2015), "Thunderstorm response spectrum: fundamentals and case study", *J. Wind Eng. Ind. Aerod.*, **143**, 62-77.
- Solari, G. and Piccardo, G. (2001), "Probabilistic 3-D turbulence modeling for gust buffeting of structures", *Prob. Eng. Mech.*, **16**(1), 73-86.
- Solari, G., Repetto, M.P., Burlando, M., De Gaetano, P., Pizzo, M., Tizzi, M. and Parodi, M. (2012), "The wind forecast for safety and management of port areas", *J. Wind Eng. Ind. Aerod.*, **104-106**, 266-277.
- Solari, G. and Tubino, F. (2002), "A turbulence model based on principal components", *Prob. Eng. Mech.*, **17**(4), 327-335.
- Vermeire, B.C., Orf, L.G. and Savory, E. (2011), "Improved modeling of downburst outflows for wind engineering applications using a cooling source approach", *J. Wind Eng. Ind. Aerod.*, **99**, 801-814.
- Wood, G.S., Kwok, K.C.S., Motteram, N.A. and Fletcher, D.F. (2001), "Physical and numerical modelling of thunderstorm downburst", *J. Wind Eng. Ind. Aerod.*, **89**, 535-552.
- Xu, Z. and Hangan, H. (2008), "Scale, boundary and inlet condition effects on impinging jets", *J. Wind Eng. Ind. Aerod.*, **96**, 2383-2402.

JH